Food Chemistry: X 23 (2024) 101634

Contents lists available at ScienceDirect

Food Chemistry: X

journal homepage: www.sciencedirect.com/journal/food-chemistry-x

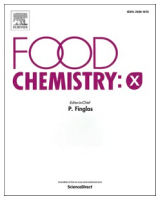

Exploration of the effects of geographical regions on the volatile and non-volatile metabolites of black tea utilizing multiple intelligent sensory technologies and untargeted metabolomics analysis

Lilei Wang [a,b], Jialing Xie [a], Yiwen Miao [b], Qiwei Wang [a], Jiajing Hu [a], Yongwen Jiang [a], Jinjin Wang [a], Huarong Tong [b], Haibo Yuan [a,*], Yanqin Yang [a,*]

[a] Key Laboratory of Biology, Genetics and breeding of Special Economic Animals and Plants, Ministry of Agriculture and Rural Affairs, Tea Research Institute, Chinese Academy of Agricultural Sciences, Hangzhou 310008, China
[b] College of Food Science, Southwest University, Beibei District, Chongqing 400715, China

ARTICLE INFO

Keywords:
Congou black tea
Geographical region
Intelligent sensory technology
Untargeted metabolomics
Multivariate statistical analysis

ABSTRACT

Geographical regions profoundly influence the flavor characteristics of Congou black tea (CBT). In this study, 35 CBT samples from 7 geographical regions were comprehensively characterized by integrated multiple intelligent sensory technologies and untargeted metabolomics analysis. A satisfactory discrimination was achieved through the fusion of multiple intelligent sensory technologies ($R^2Y = 0.918$, $Q^2 = 0.859$). A total of 104 non-volatile and 169 volatile metabolites were identified by UHPLC-HRMS and GC–MS, respectively. Of these, 45 critical differential non-volatile metabolites and 76 pivotal differential volatile metabolites were pinpointed based on variable importance in projection >1 and $p < 0.05$. Moreover, 52 key odorants with OAV ≥ 1 were identified, with hexanal, phenylacetaldehyde, linalool, β-cyclocitral, methyl salicylate, geraniol, α-ethylidene phenylacetaldehyde, and trans-β-ionone being recognized as the common odorants across 7 geographical regions. The results provide theoretical support for a comprehensive understanding of the effect of geographical regions on the flavor of black tea.

1. Introduction

Black tea, recognized as the second most produced tea in China, has gained widespread attention for its captivating aroma, sweet-mellow taste, and appealing color. In 2023, the production and sales of black tea in China reached 491.200 tons and 519.7 billions, respectively, ranking second only to green tea. The processing of Congou black tea (CBT) typically involves four fundamental steps: withering, rolling, fermentation, and drying. The tea quality is influenced by numerous factors such as geographical origin (Peng et al., 2022), cultivar (Li et al., 2022), process technology (Feng et al., 2019), altitude (Zhang, Suen, Yang, & Quek, 2018), and fertilizer (Zhao et al., 2023). Among these, geographical origin serves as one of the pivotal factors that affect consumers' choice. With the rapid development of agricultural trade globalization, the authenticity of geographical origin of tea has become increasingly prominent. Consumers generally believe that the quality of tea from the core producing regions surpasses that from conventional producing areas. However, this perception prompts businessmen to confuse origins, adulterate products and misrepresent labels in the pursuit of profitability. Thus, it is urgent to develop fast and accurate methods to identify the geographical origins of CBT and explore the key flavor compounds that influence their disparities.

Currently, traditional artificial sensory evaluation serves as the predominant method for assessing the origins and defining the flavor profile of tea, which mainly relies on subjective experience and possesses poor stability and low repeatability (Yang, Qian, Deng, Yuan, & Jiang, 2022). In order to overcome these limitations, intelligent sensory technologies have emerged as an effective solution. Representative technologies such as electronic nose (E-nose), electronic tongue (E-tongue), and electronic eye (E-eye), which mimic the human perception system, have made significant advancements in recent years (Gharibzahedi, Barba, Zhou, Wang, & Altintas, 2022; Vashisht, Pendyala, Patras, Gopisetty, & Ravi, 2022). Without complicated treatments and well-trained personnel, these advanced intelligent sensory technologies possess the capability to detect aroma, taste, and color attributes by translating their distinct sensing signals into numerical data.

* Corresponding author.
E-mail addresses: 192168092@tricaas.com (H. Yuan), yangyq@tricaas.com (Y. Yang).

https://doi.org/10.1016/j.fochx.2024.101634
Received 15 April 2024; Received in revised form 30 June 2024; Accepted 5 July 2024
Available online 6 July 2024

Their extensive applications signify the effectiveness in compensating for the inherent subjectivity and variability of human perception. For instance, the identification of geographical origin of green tea has been successfully achieved by utilizing E-nose and quantum neural network (Fu, Liu, Chen, & Xing, 2023). Similarly, the Brazilian and Indian black tea has been successfully distinguished through the integration of E-tongue coupled with multivariate statistical analysis (Raj et al., 2023). In addition, the geographical origins of tea have been validated by employing E-eye and soft independent modeling (Fernandes, Fernandes, Diniz, & Pistonesi, 2023).

Metabolomics represents a groundbreaking methodology, enabling us to gain an in-depth understanding of the regulatory mechanisms behind flavor characteristics in complex food frameworks. It is concerned with the high-throughput identification and quantification of small molecule (< 1500 Da) metabolites, facilitated by the recent groundbreaking developments in small molecule isolation and characterization techniques. Gas chromatography-mass spectrometry (GC–MS) and liquid chromatography-mass spectrometry (LC-MS) are prevalent techniques in metabolomics, and their applications have facilitated substantial advancements in the field of tea flavor (Yang et al., 2024a). Methyl salicylate, (*E*)-2-octenal, phenylacetaldehyde, linalool, and linalool oxide have been identified as the pivotal odorants in four most famous black teas (Kang et al., 2019). Epigallocatechin gallate (EGCG), possessing astringent taste, has been pinpointed as a vital non-volatile metabolite in distinguishing black teas from Kenya, Assam, Darjeeling, and Nepal (Shevchuk, Jayasinghe, & Kuhnert, 2018). Present studies focus on a particular aspect of flavor, such as aroma compounds or taste components. To offer a multidimensional and comprehensive interpretation of the effects of geographical region on CBT, intelligent sensory technology integrated with untargeted metabolomics were employed to uncover the effects of geographical region on the volatile and non-volatile metabolites of CBT.

Herein, we integrated multiple intelligent sensory technologies including gas chromatography E-nose (GC-E-Nose), E-tongue, and E-eye, along with untargeted metabolomics such as GC–MS and ultra-high performance liquid chromatography coupled to high-resolution mass spectrometry (UHPLC-HRMS), to comprehensively characterize the volatile and non-volatile metabolites of CBT originating from 7 primary regions in China. The critical metabolites for discriminating different geographical regions were screened out. The results provide a robust theoretical basis for comprehensive and in-depth understanding of geographical regions on the flavor substances of black tea.

2. Materials and methods

2.1. Materials and reagents

The 20-mL headspace vials sealed with magnetic PTFE/silicone (18 mm) were purchased from Agilent Technologies Inc. (Palo Alto, CA, USA). Purified water was acquired from Wahaha Group Co., Ltd. (Hangzhou, China). *n*-Alkane mixtures (C6-C16) were obtained from Restek Co., Ltd. (Centre County, PA, USA). Hydrochloric acid, sodium chloride, and monosodium glutamate were obtained from Alpha M.O·S., Co., Ltd. (Toulouse, France). Acetonitrile, methanol, and formic acid were purchased from Thermo Fisher Scientific (Shanghai, China).

A total of 35 CBT samples from 7 different geographical regions were used. Specifically, 5 samples were from Anhui (AH, 29°41′-34°38′ N, 114°54′-119°37′ E); 7 samples were from Fujian (FJ, 23°31′-28°18′ N, 115°50′-120°43′ E); 4 samples were from Guangdong (GD, 20°13′-25°31′ N, 109°39′-117°19′ E); 6 samples were from Hubei (HB, 29°05′-33°20′ N, 108°21′-116°07′ E); 4 samples were from Jiangxi (JX, 24°29′-30°04′ N, 113°34′-118°28′ E); 4 samples were from Sichuan (SC, 26°03′-34°19′ N, 97°21′-108°12′ E), and 5 samples were from Yunnan (YN, 21°8′-29°15′ N, 97°31′-106°11′ E).

2.2. GC-E-Nose analysis

The Heracles II GC-E-Nose system (Alpha M.O·S., Toulouse, France), which was equipped with an automated headspace sampler, was employed to gather the volatile profiles of CBT samples. Two capillary columns of MXT-5 and MXT-1701 (20 m × 0.18 mm I.D. × 0.4 μm, Restek, USA) in parallel were used. The experimental method was based on our previous study (Wang et al., 2023a). Briefly, 0.5 g of CBT samples and 3 mL of water were put into a 20-mL headspace vial, and subsequently transferred to the incubator. The incubation parameters were set at 65 °C and 500 rpm, with the entire process lasting for 30 min. After incubation, 5000 μL of headspace gas was introduced into the separation system by utilizing an airtight syringe at a flow rate of 250 μL/s for 50 s. The volatiles were concentrated via a Tenax TA trap adjusted to 40 °C for 55 s, followed by thermal desorption at 240 °C for 30 s. Helium was utilized as the carrier gas at a flow rate of 0.8 mL/min. The heating protocol was as follows: the initial temperature was set at 50 °C for 5 s, raised to 80 °C at a rate of 0.1 °C/s, and finally raised to 250 °C at a rate of 0.4 °C/s and held for 10 s. The operational temperature for the two flame ionization detectors (FIDs) was set at 260 °C. The volatile profiles were analyzed by the built-in AlphaSoft software (version 17.0), and were qualitatively evaluated by comparing the retention index calculated by C6-C16 with those in the AroChemBase database.

2.3. Electronic eye analysis

The IRIS VA400 E-eye system (Alpha M.O.S, France) was employed to collect the color information regarding CBTs. It was mainly composed of a CMOS camera (5 mm aperture), light source, cabin, and computer. Prior to image capture, it was imperative to preheat the light source, adjust the camera settings and calibrate the color. Each sample was firmly secured in the identical position within the cabin, and was captured three times. All acquired images underwent consistent preprocessing. The feature information extracted from a standardized central circle included L*a*b* values, color codes and their corresponding color regions. The L* value signifies the brightness of the infusion on a scale of 0–100, with higher values indicating greater brightness. The a* and b* values represent the redness/greenness and yellowness/blueness of the infusion, respectively, with values ranging from −128 to 127. A higher a* value denotes more redness, whereas a higher b* value signifies more yellowness.

2.4. Electronic tongue analysis

An ASTREE E-tongue system, armed with the sixth set of sensors (Alpha M.O.S, France) was utilized to gather the taste information of CBTs. This sensor array encompassed a standard reference electrode and seven taste sensors inclusive of AHS (sour), ANS (sweet), SCS (bitter), CTS (salty), NMS (umami), PKS (comprehensive taste), and CPS (comprehensive taste). Prior to measurement, the sensors were required to be activated, pre-equilibrated, calibrated, and diagnosed with the assistance of the following solutions: hydrochloric acid, sodium chloride, and sodium glutamate. During a collection sequence, a mandatory cleaning (30 s) and testing (120 s) cycle was performed. Each sample underwent a repetition of 3 times. The average value of the signal response in the period of 110th–120th s was selected as the output value, where the signal displayed consistency.

2.5. GC–MS analysis

The analysis of the volatile compounds was carried out using an Agilent 7890B—7000C GC–MS equipment (Agilent Technologies, Palo Alto, CA, USA), and the experimental method was based on our previous study (Wang et al., 2023a). Initially, 0.5 g of samples, 5 mL of water, and 2 μL of internal standard (100 mg/L, ethyl decanoate) were incorporated into a 20-mL headspace vial. A 50/30 μm divinylbenzene/carboxen/

polydimethylsiloxane (DVB/CAR/PDMS) fiber (Supelco, Bellefonte, PA, USA) was employed to extract the volatile compounds, which underwent an incubation period of 60 min at 60 °C. Each sample was prepared in triplicate. After extraction, the fiber was inserted into the injector for thermal desorption (approximately 5 min). The volatile compounds were separated via a HP-5 ms capillary column (30 m × 0.25 mm internal diameter × 0.25 μm film thickness; Agilent Technologies, Palo Alto, CA, USA). The heating protocol for the GC column was established as follows: the initial temperature was set at 40 °C (maintaining for 2 min), subsequently elevated to 160 °C at a rate of 4 °C/min (holding for 2 min), and finally progressed to 270 °C at a rate of 10 °C/min (holding for 2 min). Mass spectrometry was conducted under electron ionization mode at 70 eV. The temperatures of the injector port and transmission line were 250 °C and 270 °C, respectively. The temperature of the ion source was set at 230 °C and the mass scan range was 40–450 *m/z*.

The volatile compounds in CBTs were qualitatively assessed by the Agilent MassHunter Workstation Software, followed by a search and identification using the NIST 11 library. The volatile compounds were further confirmed with retention indices (RI), calculated through a homologous series of *n*-alkanes (C7-C40), and cross-referenced with the data available in the scientific literatures (https://webbook.nist.gov/chemistry/ and https://www.flavornet.org/flavornet.html). Each volatile was quantified employing the internal standard method.

2.6. Odor active value (OAV) analysis

Odor active value (OAV) is defined as the ratio of the concentration of volatile compound to its threshold value (Bi et al., 2019). OAV is commonly employed to assess the contribution to the overall aroma. Volatiles with an OAV ≥ 1 are recognized as the fundamental contributor to tea aroma. Moreover, the higher the OAV, the greater the contribution.

2.7. UHPLC-HRMS-based metabolomics analysis

The analysis of the non-volatile metabolites was performed utilizing an Ultimate 3000-Q-Exactive UHPLC-MS system (Thermo Fisher, CA, USA). The pre-processing approach was implemented according to previous study with minor adjustments (Han et al., 2022). Initially, 0.1 g of pre-milled tea powder was weighed and transferred into a 5-mL centrifuge tube, subsequently assorted with 3 mL methanol. After ultrasonic extraction (at 25 °C for 10 min) and centrifugation (at 4 °C for 10 min), the extracts were transferred into a centrifuge tube, and adjusted to 10 mL using methanol. Ultimately, each extract was filtered through a 0.22 μm Millipore filter for subsequent analysis.

The non-volatile metabolites were separated on an ACQUITY UPLC HSS T3 column (2.1 mm × 150 mm, 1.8 μm, Waters, MA, USA) under a temperature of 35 °C and a flow rate of 3 μL/min. The mobile phase was constituted of 0.1% vol/vol formic acid aqueous solution (mobile phase A) and 0.1% vol/vol acetonitrile formic acid solution (mobile phase B), and characterized by a gradient elution protocol: at 0–3 min, 2% B; 15 min, 100% B; 17 min, 100% B; 17.5 min, 2% B; 20 min, 2% B. The operating parameters of mass spectrometry were defined as follows: both the positive and negative ion modes were undertaken via electrospray ionization, with the ion transfer tube temperature of 320 °C and spray voltage of 3.5 kV. The temperature of auxiliary gas was maintained at 400 °C. The flow rate ratios of sheath gas and auxiliary gas were set at 40 arb and 10 arb, respectively. The scanning range was 60–900 *m/z*. Throughout the data acquisition process, quality control samples (QC) were employed to ensure the validity and consistency of acquired data. Metabolic identification was facilitated through precise mass measurements (≤ 5 ppm), retention time correction (≤ 0.2 min), peak response intensity (≥ 200,000), comparison with self-established standard databases and online database inquiries (such as HMDB 5.0).

2.8. Statistical analysis

The datasets of the GC-E-Nose, E-tongue, and E-eye were subjected to preliminary processing via their built-in workstation. Prior to modeling, the fused dataset underwent standardization through unit variance scaling (UV). Orthogonal partial least squares discrimination analysis (OPLS-DA) was performed by SIMCA 14.1 (Umetrics, Sweden). One-way analysis of variance (ANOVA) was implemented utilizing SPSS 20.0 (SPSS Inc., USA). The correlation heat map, bar plot, and bubble plot were generated using ChiPlot (https://www.chiplot.online/). The venn diagram was sketched using Omicstudio (https://www.omicstudio.cn/).

3. Results and discussion

3.1. Characterization of CBTs from different geographical regions based on multiple intelligent sensory technologies

In this study, 35 CBT samples from 7 geographical regions were characterized using GC-E-Nose, E-tongue, and E-eye. A total of 91 characteristic variables were acquired, comprising 44 variables from GC-E-Nose, 7 variables from E-tongue, and 40 variables from E-eye (Table S1). To facilitate data mining and analysis, OPLS-DA analysis was performed. The spatial distribution of these CBT samples from seven geographical regions, as determined by independent GC-E-Nose, E-tongue, and E-eye, was intuitively presented via the score plot. As illustrated in Fig. 1A, the distribution of samples from the AH, FJ, GD, JX, and YN regions were overlapped except for HB and SC regions, indicating a challenge in efficiently distinguishing CBT samples from diverse regions based on independent GC-E-Nose. The samples from FJ, GD, HB, JX, and YN regions could be effectively distinguished by E-tongue, yet an overlap persisted between AH and SC regions, suggesting that independent E-tongue was also insufficient in accomplishing this requirement (Fig. 1B). A considerable segregation was observed based on independent E-eye (Fig. 1C). Nonetheless, the aggregation degree of each region was not as satisfactory as anticipated. The permutation tests confirmed the absence of potential overfitting in the aforementioned OPLS-DA models (Fig. 1D, E and F). In conclusion, independent GC-E-nose, E-tongue, and E-eye techniques exhibit limitations in the discriminating CBT samples from distinct geographical regions. The application of fusion strategy provides a novel perspective (Xu, Wang, & Zhu, 2019).

The OPLS-DA model based on fusion of GC-E-Nose, E-tongue, and E-eye exhibited good explanatory and fitting ability ($R^2Y = 0.918$, $Q^2 = 0.859$), and the samples from 7 geographical regions were effectively separated (Fig. 2A). The AH samples were situated on the positive half of the Y-axis, whereas the FJ samples were positioned on the positive half of the X-axis. The GD and YN samples were distributed in the second quadrant and partially overlapped, potentially due to the prevalence of large leaf species in these two origins (Zheng et al., 2023). The JX samples were positioned in the fourth quadrant neighboring the negative half of the Y-axis. The SC and HB samples were stationed in the third and first quadrants, respectively. The permutation test with 200 interactions generally helps to assess the robustness of the current OPLS-DA model. The criteria for validity are that all Q^2-values to the left are lower than the original points to the right or the regression line of the Q^2-points intersects the vertical axis (on the left) at, or below zero. As illustrated in Fig. 2B, the results demonstrated that the model was reliable and not overfitted ($R^2 = 0.26$, $Q^2 = -0.526$). Additionally, a total of 29 variables were identified to play a critical role in the classification of CBTs from 7 regions based on variable importance in projection (VIP) > 1 (Fig. 2C). Among them, 15 variables were from GC-E-Nose, 7 variables were from E-tongue, and the remaining variables were from E-eye. In summary, the model based on the fusion strategy was more robust than that based on independent GC-E-Nose, E-tongue, and E-eye. This pioneering methodology enables the amalgamation of data from diverse sensory techniques, thereby enhancing the precision and

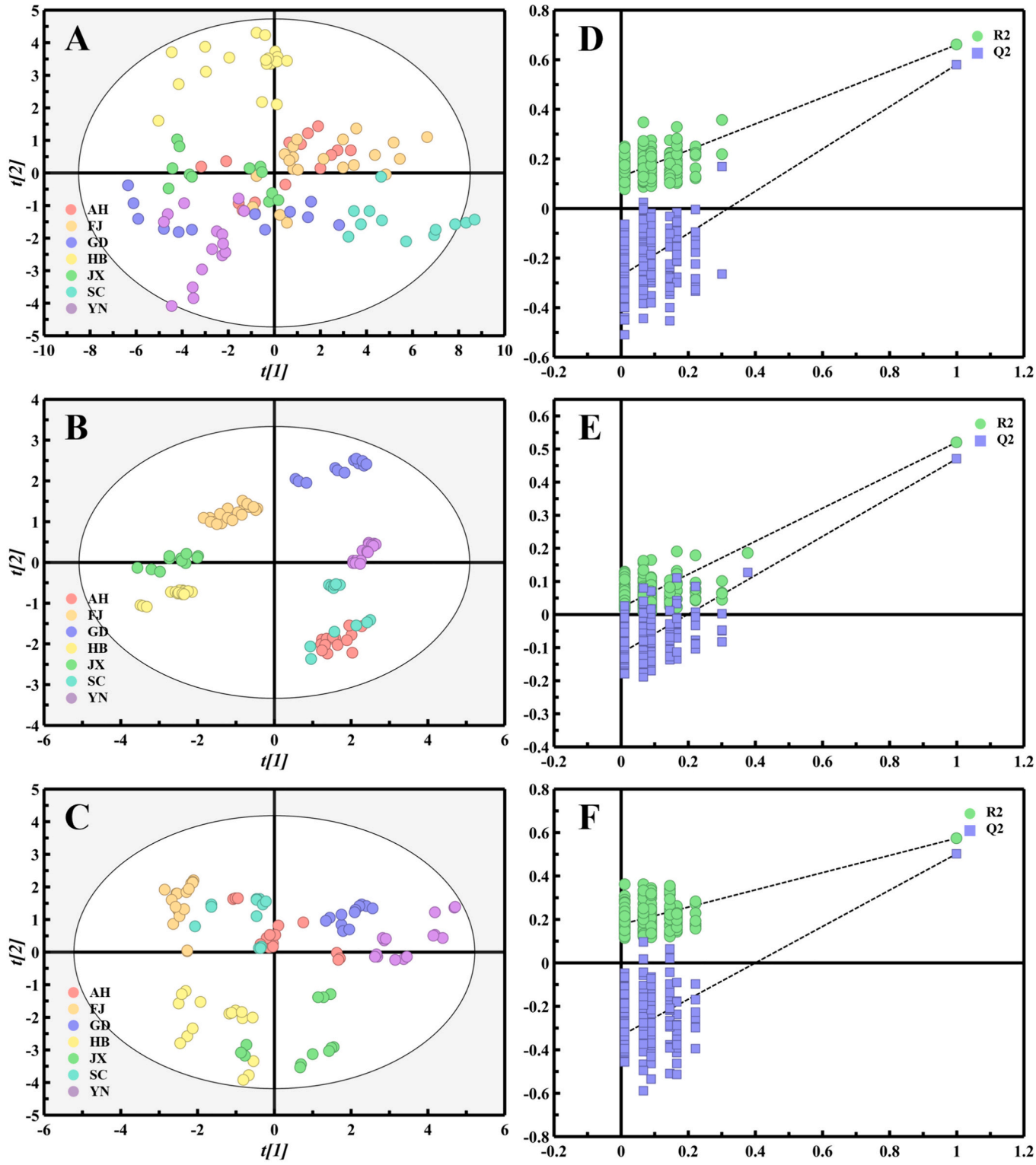

Fig. 1. OPLS-DA models based on independent GC-E-Nose, E-tongue, and E-eye. (A) Score plots of GC-E-Nose ($R^2Y = 0.641$, $Q^2 = 0.551$); (B) Score plots of E-tongue ($R^2Y = 0.643$, $Q^2 = 0.616$); (C) Score plots of E-eye ($R^2Y = 0.72$, $Q^2 = 0.673$); (D) Permutation test of GC-E-Nose ($R^2 = 0.129$, $Q^2 = -0.271$); (E) Permutation test of E-tongue ($R^2 = 0.022$, $Q^2 = -0.216$); (F) Permutation test of E-eye ($R^2 = 0.177$, $Q^2 = -0.335$). AH represents Anhui; FJ represents Fujian; GD represents Guangdong; HB represents Hubei; JX represents Jiangxi; SC represents Sichuan, and YN represents Yunnan.

dependability of the discrimination. The fusion strategy of integrating GC-E-Nose, E-tongue, and E-eye has been demonstrated as a promising methodology for distinguishing geographical regions of CBT samples. Despite intelligent sensory technologies offering the benefits of speed and objectivity, it is essential to highlight that these intelligent sensory technologies have stringent environmental requirements. Maintaining consistent environmental conditions is vital for ensuring consistent device performance. Moreover, as time progresses, sensors may encounter

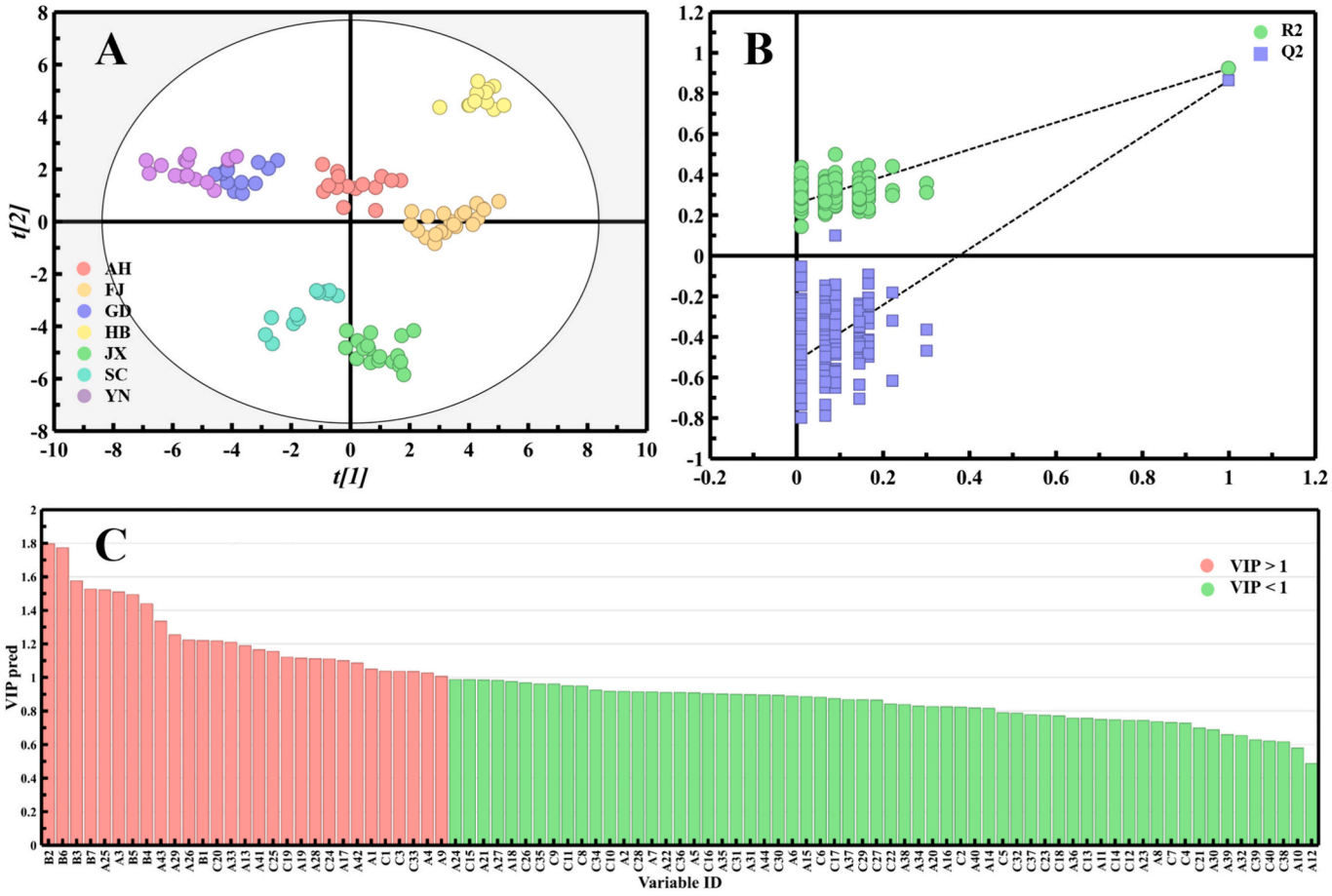

Fig. 2. OPLS-DA model based on fusion of multiple intelligent sensory technologies. (A) Score plots ($R^2Y = 0.918$, $Q^2 = 0.859$); (B) Permutation test ($R^2 = 0.26$, $Q^2 = -0.526$); (C) VIP plot. AH represents Anhui; FJ represents Fujian; GD represents Guangdong; HB represents Hubei; JX represents Jiangxi; SC represents Sichuan, and YN represents Yunnan.

performance degradation and contamination, necessitating regular replacement of the sensor or rigorous cleaning protocols to maintain the sensor cleanliness. Nevertheless, they remain a convenient method for evaluating the quality of black tea.

3.2. Characterization of the non-volatile metabolites in CBTs from different geographical regions based on UHPLC-HRMS analysis

An untargeted metabolomics analysis based on UHPLC-HRMS was performed to characterize the non-volatile metabolites of CBTs from 7 geographical regions. In total, 104 non-volatile metabolites classified into 10 categories were identified, including 6 alkaloids, 19 amino acids and derivatives, 8 catechins, 9 dimeric catechins, 29 flavonol and flavonol/flavone glycosides, 5 carbohydrates, 6 nucleosides and nucleotides, 3 organic acids, 14 phenolic acids and derivatives and 5 other compounds (as detailed in Table S2).

To explore the differences of non-volatile metabolites, an OPLS-DA analysis was conducted. As illustrated in Fig. 3A, the score plots exhibited a distinct clustering tendency of CBT samples from various geographical regions, particularly exhibiting a high degree of intra-group aggregation across all groups ($R^2Y = 0.923$, $Q^2 = 0.869$). The AH, SC, and JX samples were grouped jointly in the 1st quadrant; FJ and HB samples were distributed within the 3rd quadrant; whereas GD and YN samples were located in the 4th quadrant. Notably, the close distribution of GD and YN samples was also evident in Fig. 2A, which corroborated the aforementioned results. Permutation test with 200 interactions validated the reliability of this model ($R^2 = 0.305$, $Q^2 = -0.574$) (Fig. 3B). Subsequently, a VIP plot was developed to screen the potential key non-volatile metabolites responsible for quality differences between regions. A total of 45 non-volatile metabolites were selected based on the criterion of VIP > 1 and $p < 0.05$ (Fig. 3C). The top five non-volatile metabolites with VIP > 1.3 were kynurenic acid (L1), (−)-asparagine (L10), procyanidin B1 (L35), naringenin (L51), and adenine (L75), contributing substantially to the differences. Consequently, these pivotal differential non-volatile metabolites were highlighted in the loading plot to elucidate their specific contribution to the quality differences between regions (Fig. 3D). The closer the metabolite resided to the cluster, the more sensitive it was to the classification. (−)-Asparagine (L10), imparting an umami taste, was closer to the YN and GD groups while L-isoleucine (L19) were proximate to the HB and FJ groups (Yang et al., 2018). Fumaric acid (L84) was located near the GD and YN samples. It contributed to form a mellow and thick flavor, and was reported to exhibit a considerable distinction between large-leaf black tea and medium-small-leaf black tea (Song et al., 2020).

Furthermore, a heat map was utilized to visualize the distribution patterns of key differential metabolites across 7 geographical regions (Fig. 4). Each circle represents a region, while each column represents a compound. The orange box indicates a higher level than the average, whereas the cyan box signifies a lower level. The CBT samples could be categorized into two dominant categories: the medium-small-leaf species group encompassed AH, FJ, HB, JX, and SC; the large-leaf species group included YN and GD. It is worth mentioning that, the former group could be further subdivided into two subcategories: AH, JX, and SC; FJ and HB. The results demonstrate the potential of UHPLC-HRMS in elucidating the quality differences between diverse regions.

Upon scrutinizing the non-volatile metabolites, there existed seven

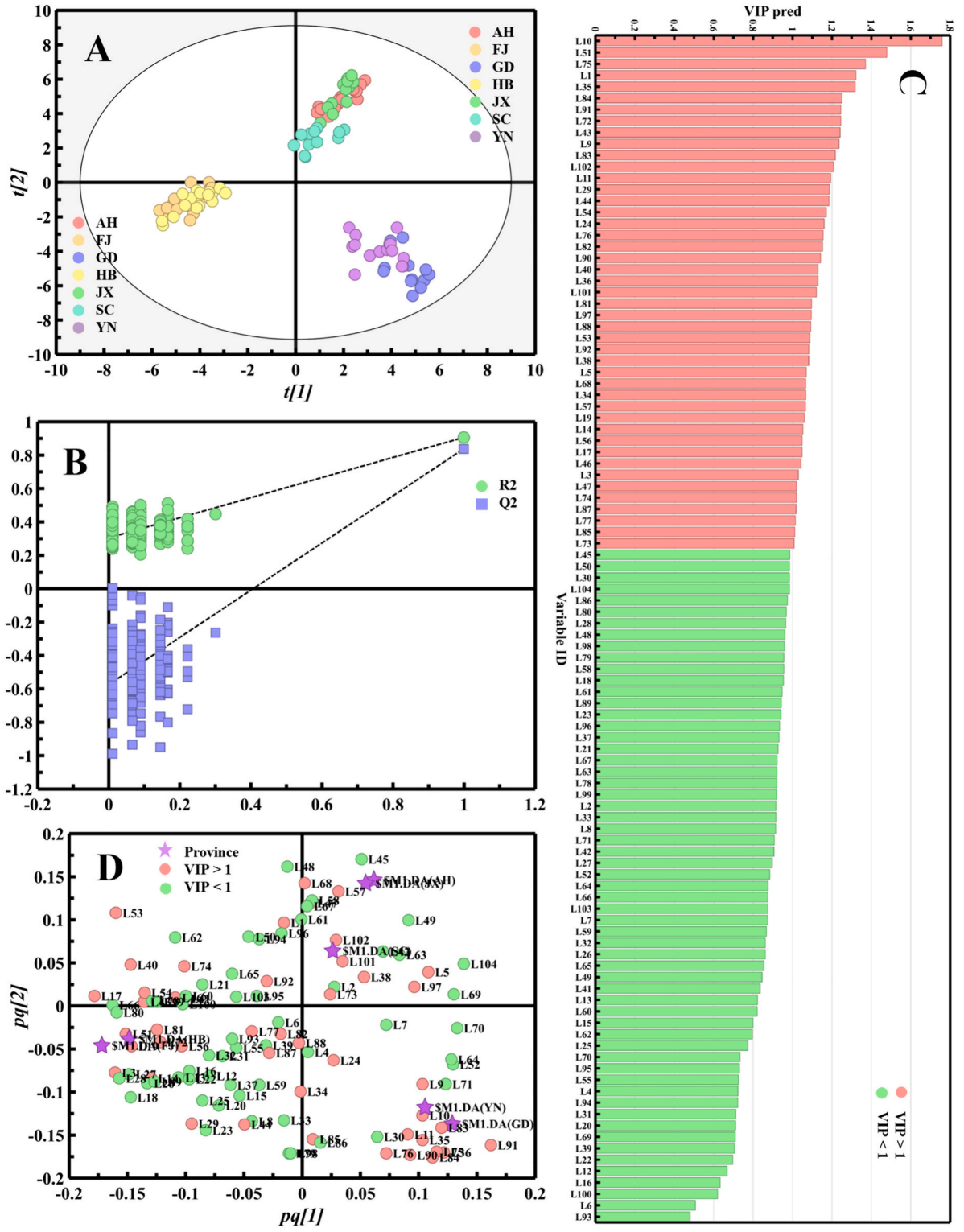

Fig. 3. OPLS-DA model based on UHPLC-HRMS. (A) Scores plot ($R^2Y = 0.923$, $Q^2 = 0.869$); (B) Permutation test ($R^2 = 0.305$, $Q^2 = -0.574$); (C) VIP plot; (D) Loading plot. AH represents Anhui; FJ represents Fujian; GD represents Guangdong; HB represents Hubei; JX represents Jiangxi; SC represents Sichuan, and YN represents Yunnan.

distinct metabolite clustering blocks that played an important role in discriminating different regions of CBTs. Cluster I was primarily consisted of amino acids and dimeric catechins with umami and astringent tastes, such as (−)-asparagine and procyanidin B1 (Wu et al., 2022). These metabolites predominantly exhibited higher levels in the YN samples. Cluster II was consisted of four carbohydrates and one phenolic acid, displaying greater levels in the GD samples. These carbohydrates not only significantly contribute to the sweet taste of black tea, but they also act as substantial contributors to the mouth feel of the infusion (Zhang et al., 2023a). Three organic acids in cluster III displayed higher

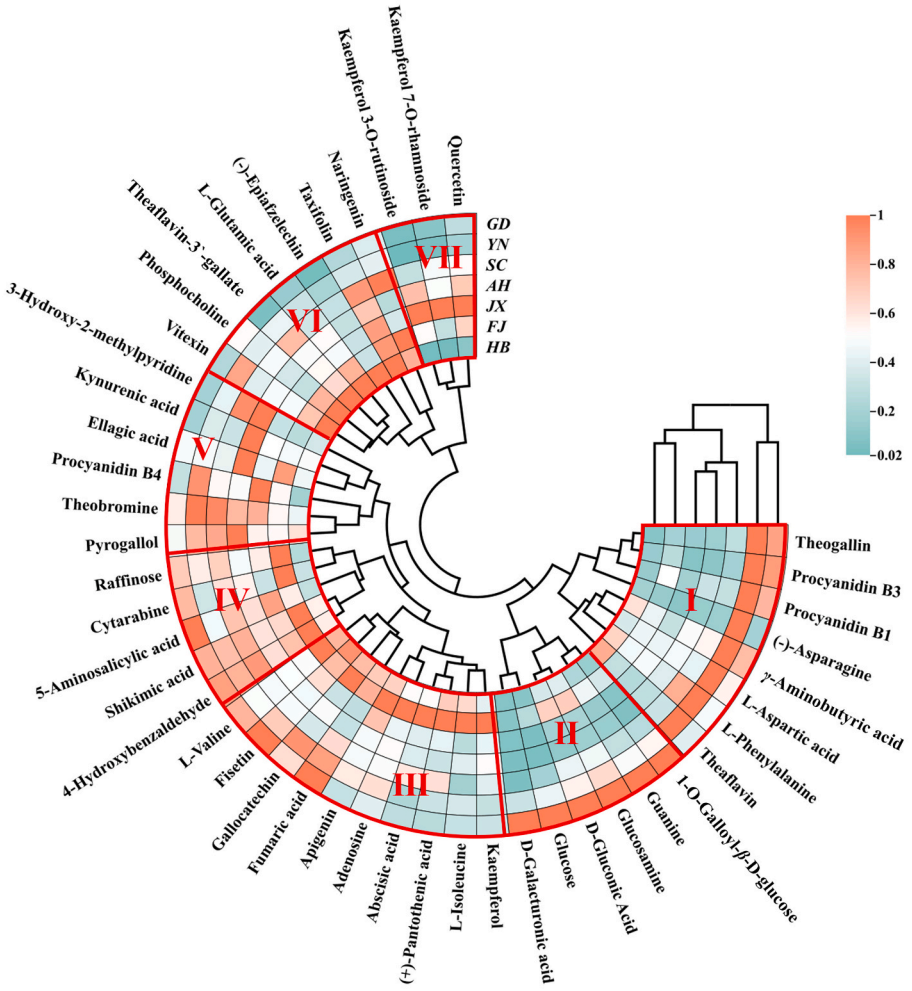

Fig. 4. Heat map of key differential non-volatile metabolites in CBTs from 7 geographical regions. AH represents Anhui; FJ represents Fujian; GD represents Guangdong; HB represents Hubei; JX represents Jiangxi; SC represents Sichuan, and YN represents Yunnan.

levels in the FJ samples compared to other groups. Cluster IV was composed of 4-hydroxybenzaldehyde, shikimic acid, 5-aminosalicylic acid, cytarabine, and raffinose. In addition, kynurenic acid, theobromine, procyanidin B4, ellagic acid, pyrogallol, and 3-hydroxy-2-methylpyridine were categorized within cluster V, demonstrating higher levels in the AH samples. Flavonol/flavone and their glycosides were the primary substances in clusters VI and VI, predominantly exhibiting astringent taste and contributing greatly to the formation of black tea flavor (Ito & Yanase, 2022).

3.3. Characterization of the volatile metabolites in CBTs from different geographical regions based on GC–MS

In this study, GC–MS was employed to investigate the volatile metabolites in CBTs from different geographical regions. A total of 169 volatile metabolites were identified within 7 geographical regions of CBT samples (as detailed in Table S3). Based on their chemical structures, these volatile metabolites could be sub-grouped into 12 categories, consisting of 27 alcohols, 30 aldehydes, 28 ketones, 30 esters, 19 heterocyclic compounds, 15 alkenes, 9 aromatic hydrocarbons, 5 acids, 2 alkanes, 2 sulfides, 1 phenol, and 1 ether. With respect to individual region, there were 60, 71, 48, 88, 58, 73, and 47 volatile metabolites identified in the AH, FJ, GD, HB, JX, SC, and YN, respectively (Fig. S1). Moreover, the contents of volatile metabolites varied across diverse regions (Fig. S2). High levels of alcohols, aldehydes, and esters were detected in all regions, corroborating previous study (Xiao et al., 2017). Remarkably, elevated levels of esters and alkenes were detected in FJ samples, which emitted floral and fruity aromas. The SC samples contained higher levels of ketones, aldehydes, and alcohols. Interestingly, sulfides, phenols, and ethers were exclusively observed in the HB samples.

An OPLS-DA analysis was carried out to investigate the key volatile metabolites that contributed to the quality differences in geographic regions. As depicted in Fig. 5A, 7 geographical regions of CBT samples were well distinguished, exhibiting commendable explanatory power and predictive potential (R^2 Y = 0.928, Q^2 = 0.902). The FJ and HB samples were distributed in the third and fourth quadrants, respectively. The remaining five regions (i.e., AH, GD, JX, SC, and YN) were located in the first quadrant near the positive half of the Y-axis, indicating similar volatile metabolites across these five regions. Permutation testing for 200 interactions confirmed the model's reliability devoid of overfitting (Fig. 5B). According to the criteria of VIP >1 and $p < 0.05$, 76 volatile metabolites were recognized as key contributors towards discriminating CBTs from 7 geographical regions (Fig. 5C). Subsequent assessment of specific volatile metabolites interpreting the diversity across seven geographical regions was performed via the corresponding loading plots (Fig. 5D). The separation distance between individual variables and the primary cluster positively correlates with their contribution to classification. For instance, (*Z*)-3-hexen-1-ol acetate (G48), (*E*)-linalool oxide (pyranoid) (G93), *β*-ocimene (G61), geraniol (G115), *β*-myrcene (G41), and hexadecanoic acid ethyl ester (G169) were closer to the FJ region. Geraniol, possessing a rose-like aroma, was one of the typical volatile

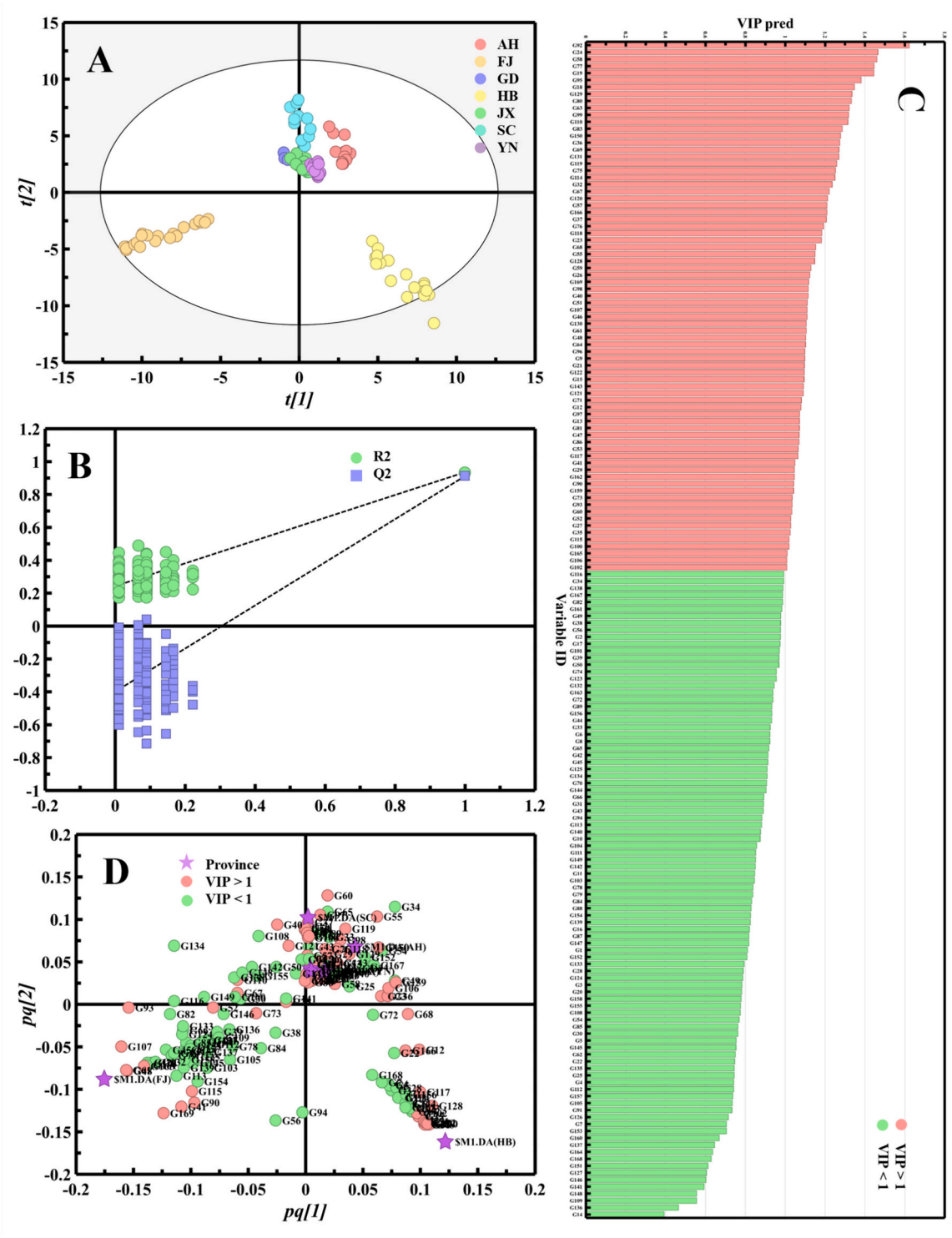

Fig. 5. OPLS-DA model based on GC–MS. (A) Score plots ($R^2Y = 0.928$, $Q^2 = 0.902$); (B) Permutation test ($R^2 = 0.243$, $Q^2 = -0.399$); (C) VIP plot; (D) Loading plot. AH represents Anhui; FJ represents Fujian; GD represents Guangdong; HB represents Hubei; JX represents Jiangxi; SC represents Sichuan, and YN represents Yunnan.

metabolites of fresh black tea. It was hydrolyzed from *β*-D-glycosides (Polat, Şat, & Ilgaz, 2018). Hexanoic acid ethyl ester (G46), terpinolene (G71), nerol (G117), and thymol (G128) were adjacent to the HB region, while 1-hexanol (G19), 2-ethyl-pyrazine (G29), 2-pentyl-furan (G40), benzeneacetaldehyde (G57), and (*E*)-2-octenal (G63) were distributed around the remaining regions. Esters typically impart a fruity or floral aroma to black tea. As a typical representative, hexanoic acid ethyl ester was generated through lipid oxidation and degradation, and was the primary aroma compound of Yingde black tea (Liu et al., 2021; Wang et al., 2023b). 2-Pentyl-furan, derived from the Maillard reaction via Strecker degradation, was reported as an important aroma-active component in black tea, green tea, and white tea (Hao et al., 2023; Ouyang et al., 2022; Su, He, Zhou, Li, & Zhou, 2022).

Typically, aroma is shaped by diverse volatile compounds through comprehensive and complex interaction. OAV analysis was performed to identify the key aroma compounds in CBT samples from 7 geographical regions. A total of 52 volatile compounds with OAV ≥ 1 were screened out in all regions (Table S4). Specifically, there were 21, 31, 21, 24, 22,

31, and 18 key odorants identified in AH, FJ, GD, HB, JX, SC, and YN, respectively (Fig. 6). For instance, theaspirane (OAV = 17,000) and 2,3-diethyl-5-methyl-pyrazine (OAV = 25.8) were exclusively found in AH region; (*Z*)-3-Hexen-1-ol acetate (OAV = 1.2), *β*-ocimene (OAV = 2.5), 1,3,8-p-menthatriene (OAV = 37), dihydro-5-pentyl-2(3H)-furanone (OAV = 1.2), and cedrol (OAV = 8.8) were exclusively found in FJ region; Hexanoic acid, ethyl ester (OAV = 1.5), dimethyl trisulfide (OAV = 5), 2-ethyl-furan (OAV = 4.5), and 3-methyl-butanal (OAV = 53.1) were exclusively found in HB region; 1-Hexanol (OAV = 2.8) was exclusively found in JX region; *α*-Phellandrene (OAV = 23) and 2-ethyl-5-methyl-pyrazine (OAV = 2) were exclusively found in SC region; 2,6-Dimethyl-2,4,6-octatriene (OAV = 9860) was exclusively found in YN region. The aforementioned volatile compounds potentially contributed to the differing aroma qualities of CBTs from 7 geographical regions. Teaspirane was considered as a potential marker for distinguishing Wuyi rock tea cultivars (Zhang et al., 2023b). 2,6-Dimethyl-2,4,6-octatriene, contributing to a floral aroma, was documented to exhibit a higher level in high-quality Bao-Chung tea (Chen, Liu, & Chen, 2023). It is noteworthy that 1-octen-3-ol (excluding AH), (*E*)-linalool oxide (pyranoid) (excluding HB), and *β*-damascenone (excluding HB) were detected in almost all regions. 1-Octen-3-ol and *β*-damascenone could be regulated through distinct withering methods, and significantly influenced the formation of black tea aroma (Huang et al., 2022). trans-Linalool oxide (pyranoid) was reported to have a positive impact on the aroma profile of Yunnan CBTs, and was an essential indicator to distinguish diverse roasting periods (Mei et al., 2022).

In addition, 8 volatile compounds including hexanal, phenylacetaldehyde, linalool, *β*-cyclocitral, methyl salicylate, geraniol, *α*-ethylidene phenylacetaldehyde, and trans-*β*-ionone were identified as common odorants in CBT samples from 7 geographical regions (Fig. S3). Notably, trans-*β*-ionone and methyl salicylate were recognized as the constructors of the fundamental aroma of black tea. Their contents did not exhibit considerable disparity across the seven regions, suggesting that they merely contribute to the foundational aroma rather than serving as the determinant of the aroma distinction. Linalool and geraniol were reported to impart a floral aroma, whereas phenylacetaldehyde emitted a honey-like aroma. Both of them were identified as highly associated with the sweetness and floral aromas of CBTs. Hexanal exhibited a grassy odor, and its content was relatively low in high-quality black tea (Gao et al., 2022). *β*-Cyclocitral, exhibiting a fruity fragrance, was regarded as potential aroma-active component responsible for sweet aroma black tea (Yang et al., 2024b). *α*-Ethylidene phenylacetaldehyde was reported to be closely linked to the honey-like attribute (Sun et al., 2024).

4. Conclusions

This study comprehensively assessed the characteristic quality of CBTs from seven diverse geographical regions by employing multiple intelligent sensory and untargeted metabolomics analysis. Exceptional differentiation was accomplished via amalgamation of multiple intelligent sensory techniques encompassing GC-E-Nose, E-tongue, and E-eye ($R^2Y = 0.918$, $Q^2 = 0.859$). A total of 45 non-volatile metabolites were identified as the key differential metabolites for distinguishing CBTs from 7 distinct regions, with screening criterion of VIP > 1 and $p < 0.05$. Both OPLS-DA and cluster analysis of non-volatile metabolites underscored the distinct disparities of CBTs between large-leaf species (GD and YN) and medium-small-leaf species (AH, FJ, HB, JX, and SC). Furthermore, 52 key odorants with OAV ≥ 1 were identified, with AH, FJ, GD, HB, JX, SC, and YN region containing 21, 21, 21, 24, 22, 31, and 18 odorants, respectively. These volatiles played a crucial role in shaping the distinctive aroma profiles of CBTs from diverse regions. Among them, hexanal, phenylacetaldehyde, linalool, *β*-cyclocitral, methyl salicylate, geraniol, *α*-ethylidene phenylacetaldehyde, and trans-

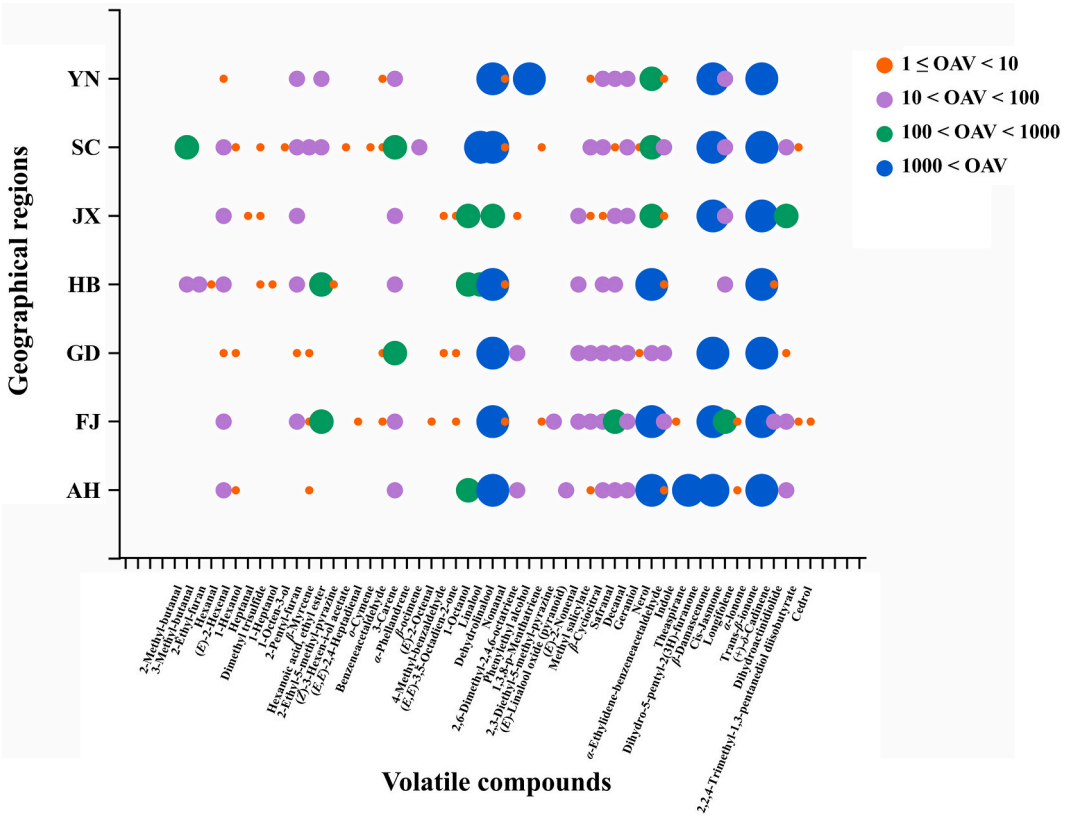

Fig. 6. Bubble plot of volatile compounds with OAV ≥ 1. AH represents Anhui; FJ represents Fujian; GD represents Guangdong; HB represents Hubei; JX represents Jiangxi; SC represents Sichuan, and YN represents Yunnan.

β-ionone were considered as the fundamental aromas across seven regions. Our results provide a thorough comprehension of the formation of CBT quality differences from various regions. In the future, we aim to explore the application of advanced data fusion methods and intelligent classification algorithms to improve the accuracy of origin classification. In addition, aroma recombination and omission testing will be conducted to gain a comprehensive understanding of the contributions of individual aroma compound.

CRediT authorship contribution statement

Lilei Wang: Writing – original draft, Visualization, Validation, Software, Methodology, Investigation, Formal analysis, Data curation. **Jialing Xie:** Methodology, Formal analysis. **Yiwen Miao:** Software. **Qiwei Wang:** Formal analysis. **Jiajing Hu:** Formal analysis, Validation. **Yongwen Jiang:** Project administration, Funding acquisition. **Jinjin Wang:** Resources. **Huarong Tong:** Conceptualization. **Haibo Yuan:** Supervision, Project administration, Funding acquisition. **Yanqin Yang:** Writing – review & editing, Visualization, Validation, Methodology, Conceptualization.

Declaration of competing interest

The authors declare that they have no known competing financial interests or personal relationships that could have appeared to influence the work reported in this paper.

Data availability

Data will be made available on request.

Acknowledgments

This work was supported by Zhejiang Provincial Natural Science Foundation of China (Grant No. LY24C160002), China Agriculture Research System of MOF and MARA (No. CARS-19), and the Science and Technology Innovation Project of the Chinese Academy of Agricultural Sciences (CAAS-ASTIP-TRICAAS).

Appendix A. Supplementary data

Supplementary data to this article can be found online at https://doi.org/10.1016/j.fochx.2024.101634.

References

Bi, S., Wang, A., Wang, Y., Xu, X., Luo, D., Shen, Q., & Wu, J. (2019). Effect of cooking on aroma profiles of Chinese foxtail millet (*Setaria italica*) and correlation with sensory quality. *Food Chemistry, 289*, 680–692. https://doi.org/10.1016/j.foodchem.2019.03.108

Chen, P.-A., Liu, C.-I., & Chen, K.-R. (2023). Determining the relationship between aroma and quality of Bao-Chung tea by solid-phase microextraction (SPME) and electronic nose analyses. *Horticulturae, 9*(8), 930. https://doi.org/10.3390/horticulturae9080930

Feng, Z., Li, Y., Li, M., Wang, Y., Zhang, L., Wan, X., & Yang, X. (2019). Tea aroma formation from six model manufacturing processes. *Food Chemistry, 285*, 347–354. https://doi.org/10.1016/j.foodchem.2019.01.174

Fernandes, J. S., Fernandes, D. D. D., Diniz, P. H. G. D., & Pistonesi, M. F. (2023). Tea authentication and determination of chemical constituents using digital image-based fingerprint signatures and chemometrics. *Food Chemistry, 421*, Article 136164. https://doi.org/10.1016/j.foodchem.2023.136164

Fu, J., Liu, R., Chen, Y., & Xing, J. (2023). Discrimination of geographical indication of Chinese green teas using an electronic nose combined with quantum neural networks: A portable strategy. *Sensors and Actuators B: Chemical, 375*, Article 132946. https://doi.org/10.1016/j.snb.2022.132946

Gao, C., Huang, Y., Li, J., Lyu, S., Wang, Z., Xie, F., … Sun, W. (2022). Relationship between the grade and the characteristic flavor of PCT (Panyong Congou black tea). *Foods, 11*(18), 2815. https://doi.org/10.3390/foods11182815

Gharibzahedi, S. M. T., Barba, F. J., Zhou, J., Wang, M., & Altintas, Z. (2022). Electronic sensor technologies in monitoring quality of tea: A review. *Biosensors, 12*(5), 356. https://doi.org/10.3390/bios12050356

Han, Z., Wen, M., Zhang, H., Zhang, L., Wan, X., & Ho, C.-T. (2022). LC-MS based metabolomics and sensory evaluation reveal the critical compounds of different grades of Huangshan Maofeng green tea. *Food Chemistry, 374*, Article 131796. https://doi.org/10.1016/j.foodchem.2021.131796

Hao, Z., Feng, J., Chen, Q., Lin, H., Zhou, X., Zhuang, J., … Yu, B. (2023). Comparative volatiles profiling in milk-flavored white tea and traditional white tea Shoumei via HS-SPME-GC-TOFMS and OAV analyses. *Food Chemistry: X, 18*, Article 100710. https://doi.org/10.1016/j.fochx.2023.100710

Huang, W., Fang, S., Wang, J., Zhuo, C., Luo, Y., Yu, Y., … Ning, J. (2022). Sensomics analysis of the effect of the withering method on the aroma components of Keemun black tea. *Food Chemistry, 395*, Article 133549. https://doi.org/10.1016/j.foodchem.2022.133549

Ito, A., & Yanase, E. (2022). Study into the chemical changes of tea leaf polyphenols during japanese black tea processing. *Food Research International, 160*, Article 111731. https://doi.org/10.1016/j.foodres.2022.111731

Kang, S., Yan, H., Zhu, Y., Liu, X., Lv, H. P., Zhang, Y., … Lin, Z. (2019). Identification and quantification of key odorants in the world's four most famous black teas. *Food Research International, 121*, 73–83. https://doi.org/10.1016/j.foodres.2019.03.009

Li, Y., Ran, W., He, C., Zhou, J., Chen, Y., Yu, Z., & Ni, D. (2022). Effects of different tea tree varieties on the color, aroma, and taste of Chinese Enshi green tea. *Food Chemistry: X, 14*, Article 100289. https://doi.org/10.1016/j.fochx.2022.100289

Liu, H., Xu, Y., Wen, J., An, K., Wu, J., Yu, Y., … Guo, M. (2021). A comparative study of aromatic characterization of Yingde black tea infusions in different steeping temperatures. *LWT- Food Science and Technology, 143*, Article 110860. https://doi.org/10.1016/j.lwt.2021.110860

Mei, S., Cao, Y., Zhang, G., Zhou, S., Wang, Y., Gong, S., … Chen, P. (2022). Construction of sensory/mass spectrometry feedback platform for seeking aroma contributors during the aroma enhancement of Congou black tea. *Plants (Basel), 11*(6), 823. https://doi.org/10.3390/plants11060823

Ouyang, W., Yu, Y., Wang, H., Jiang, Y., Hua, J., Ning, J., & Yuan, H. (2022). Analysis of volatile metabolite variations in strip green tea during processing and effect of rubbing degree using untargeted and targeted metabolomics. *Food Research International, 162*, Article 112099. https://doi.org/10.1016/j.foodres.2022.112099

Peng, C.-Y., Ren, Y.-F., Ye, Z.-H., Zhu, H.-Y., Liu, X.-Q., Chen, X.-T., … Cai, H.-M. (2022). A comparative UHPLC-Q/TOF-MS-based metabolomics approach coupled with machine learning algorithms to differentiate Keemun black teas from narrow-geographic origins. *Food Research International, 158*, Article 111512. https://doi.org/10.1016/j.foodres.2022.111512

Polat, A., Şat, İ. G., & Ilgaz, Ş. (2018). Comparison of black tea volatiles depending on the grades and different drying temperatures. *Journal of Food Processing and Preservation, 42*(7), Article e13653. https://doi.org/10.1111/jfpp.13653

Raj, D. R. K., Ferreira, M. V.d. S., Braunger, M. L., Riul, A., Thomas, J., & Barbin, D. F. (2023). Exploration of an impedimetric electronic tongue and chemometrics for characterization of black tea from different origins. *Journal of Food Composition and Analysis, 123*, Article 105535. https://doi.org/10.1016/j.jfca.2023.105535

Shevchuk, A., Jayasinghe, L., & Kuhnert, N. (2018). Differentiation of black tea infusions according to origin, processing and botanical varieties using multivariate statistical analysis of LC-MS data. *Food Research International, 109*, 387–402. https://doi.org/10.1016/j.foodres.2018.03.059

Song, C., Fan, F., Gong, S., Guo, H., Li, C., & Zong, B. (2020). Taste characteristic and main contributing compounds of different origin black tea. *Scientia Agricultura Sinica, 53*(2), 383–394. https://doi.org/10.3864/j.issn.0578-1752.2020.02.012

Su, D., He, J. J., Zhou, Y. Z., Li, Y. L., & Zhou, H. J. (2022). Aroma effects of key volatile compounds in Keemun black tea at different grades: HS-SPME-GC-MS, sensory evaluation, and chemometrics. *Food Chemistry, 373*, Article 131587. https://doi.org/10.1016/j.foodchem.2021.131587

Sun, Z., Lin, Y., Yang, H., Zhao, R., Zhu, J., & Wang, F. (2024). Characterization of honey-like characteristic aroma compounds in Zunyi black tea and their molecular mechanisms of interaction with olfactory receptors using molecular docking. *LWT-Food Science and Technology, 191*, Article 115640. https://doi.org/10.1016/j.lwt.2023.115640

Vashisht, P., Pendyala, B., Patras, A., Gopisetty, V. V. S., & Ravi, R. (2022). Design and efficiency evaluation of a mid-size serpentine dean flow UV-C system for the processing of whole milk using computational fluid dynamics and biodosimetry. *Journal of Food Engineering, 335*, Article 111168. https://doi.org/10.1016/j.jfoodeng.2022.111168

Wang, J., Ouyang, W., Zhu, X., Jiang, Y., Yu, Y., Chen, M., … Hua, J. (2023b). Effect of shaking on the improvement of aroma quality and transformation of volatile metabolites in black tea. *Food Chemistry, X, 20,*, 101007. https://doi.org/10.1016/j.fochx.2023.101007

Wang, L., Xie, J., Deng, Y., Jiang, Y., Tong, H., Yuan, H., & Yang, Y. (2023a). Volatile profile characterization during the drying process of black tea by integrated volatolomics analysis. *LWT-Food Science and Technology, 184*, 115039. https://doi.org/10.1016/j.lwt.2023.115039

Wu, S., Yu, Q., Shen, S., Shan, X., Hua, J., Zhu, J., … Li, J. (2022). Non-targeted metabolomics and electronic tongue analysis reveal the effect of rolling time on the sensory quality and nonvolatile metabolites of congou black tea. *LWT- Food Science and Technology, 169*, Article 113971. https://doi.org/10.1016/j.lwt.2022.113971

Xiao, Z., Wang, H., Niu, Y., Liu, Q., Zhu, J., Chen, H., & Ma, N. (2017). Characterization of aroma compositions in different Chinese congou black teas using GC-MS and GC-O combined with partial least squares regression. *Flavour and Fragrance Journal, 32*(4), 265–276. https://doi.org/10.1002/ffj.3378

Xu, M., Wang, J., & Zhu, L. (2019). The qualitative and quantitative assessment of tea quality based on E-nose, E-tongue and E-eye combined with chemometrics. *Food Chemistry, 289*, 482–489. https://doi.org/10.1016/j.foodchem.2019.03.080

Yang, C., Hu, Z., Lu, M., Li, P., Tan, J., Chen, M., … Lin, Z. (2018). Application of metabolomics profiling in the analysis of metabolites and taste quality in different subtypes of white tea. *Food Research International, 106*, 909–919. https://doi.org/10.1016/j.foodres.2018.01.069

Yang, Y., Qian, M. C., Deng, Y., Yuan, H., & Jiang, Y. (2022). Insight into aroma dynamic changes during the whole manufacturing process of chestnut-like aroma green tea by combining GC-E-Nose, GC-IMS, and GC × GC-TOFMS. *Food Chemistry, 387*, Article 132813. https://doi.org/10.1016/j.foodchem.2022.132813

Yang, Y., Xie, J., Wang, Q., Deng, Y., Zhu, L., Zhu, J., … Jiang, Y. (2024b). Understanding the dynamic changes of volatile and non-volatile metabolites in black tea during processing by integrated volatolomics and UHPLC-HRMS analysis. *Food Chemistry, 432*, 137124. https://doi.org/10.1016/j.foodchem.2023.137124

Yang, Y., Xie, J., Wang, Q., Wang, L., Shang, Y., Jiang, Y., & Yuan, H. (2024a). Volatolomics-assisted characterization of the key odorants in green off-flavor black tea and their dynamic changes during processing. *Food Chemistry: X, 22*, Article 101432. https://doi.org/10.1016/j.fochx.2024.101432

Zhang, C., Suen, C. L.-C., Yang, C., & Quek, S. Y. (2018). Antioxidant capacity and major polyphenol composition of teas as affected by geographical location, plantation elevation and leaf grade. *Food Chemistry, 244*, 109–119. https://doi.org/10.1016/j.foodchem.2017.09.126

Zhang, M., Zhou, C., Zhang, C., Xu, K., Lu, L., Huang, L., … Guo, Y. (2023a). Analysis of characteristics in the macro-composition and volatile compounds of understory Xiaobai white tea. *Plants, 12*(24), 4102. https://doi.org/10.3390/plants12244102

Zhang, Y., Zhang, Y.-H., Yan, H., Shao, C.-Y., Li, W.-X., Lv, H.-P., … Zhu, Y. (2023b). Enantiomeric separation and precise quantification of chiral volatiles in Wuyi rock teas using an efficient enantioselective GC×GC-TOFMS approach. *Food Research International, 169*, 112891. https://doi.org/10.1016/j.foodres.2023.112891

Zhao, S., Bai, Y., Jin, Z., Long, L., Diao, W., Chen, W., … Tang, D. (2023). Effects of the combined application of nitrogen and selenium on tea quality and the expression of genes involved in nitrogen uptake and utilization in tea cultivar 'Chuancha No.2'. *Agronomy, 13*(12), 2997. https://doi.org/10.3390/agronomy13122997

Zheng, F., Gan, S., Zhao, X., Chen, Y., Zhang, Y., Qiu, T., … Dai, Q. (2023). Unraveling the chemosensory attributes of Chinese black teas from different regions using GC-IMS combined with sensory analysis. *LWT- Food Science and Technology, 184*, Article 114988. https://doi.org/10.1016/j.lwt.2023.114988